Evaluation of Brain Metabolism in Steno-Occlusive Carotid Artery Disease by Proton MR Spectroscopy: A Correlative Study with Oxygen Metabolism by PET

Chika Tsuchida, Hirohiko Kimura, Norihiro Sadato, Tatsuro Tsuchida, Yasuhiko Tokuriki, and Yoshiharu Yonekura

Department of Radiology and Biomedical Imaging Research Center, Fukui Medical University, Fukui; Department of Neurosurgery, Fukui Red Cross Hospital, Fukui; and Department of Cerebral Research, National Institute for Neurological Sciences, Okazaki, Japan

Carotid occlusive diseases may cause ischemic changes in both the gray matter and the white matter as a result of hemodynamic compromise. To validate the use of proton magnetic resonance spectroscopy (MRS) in evaluating the carotid occlusive diseases, we compared changes in peaks of choline, in the sum of creatine and phosphocreatine, and in *N*-acetyl-aspartate (NAA) of the white matter with cortical oxygen metabolism measured by PET. **Methods:** Eleven patients with unilateral steno-occlusive carotid artery disease underwent PET and MRS. Ten age-matched healthy volunteers underwent MRS. No subjects had cortical infarction. MRS was performed bilaterally in the centrum semiovale. Regional blood flow, regional metabolic rate of oxygen ($rCMRO_2$), and regional oxygen extraction fraction (rOEF) of the cerebral cortex were measured by the steady-state method with ^{15}O gas. **Results:** The asymmetry index of the ratio of NAA to the sum of creatine and phosphocreatine (NAA/Cr) correlated positively with the asymmetry index of $rCMRO_2$ ($r = 0.77$; $P < 0.01$). Because $rCMRO_2$ is a marker of tissue viability, the NAA/Cr of the centrum semiovale may reflect viable neuronal cells. The asymmetry index of the ratio of choline to the sum of creatine and phosphocreatine (Cho/Cr) showed a significant positive correlation with the asymmetry index of rOEF ($r = 0.65$; $P < 0.05$). All but 1 patient with an increased Cho/Cr (>1.03) showed an increase in rOEF of the ipsilateral cortex (>0.56). This finding may indicate membrane damage caused by ischemia, because the centrum semiovale is the deep watershed zone. **Conclusion:** The metabolic changes in the centrum semiovale detected by proton MRS reflect a hemodynamically compromised state and are useful in evaluating tissue viability.

Key Words: magnetic resonance spectroscopy; emission tomography; carotid artery diseases; cerebral ischemia; oxygen metabolism

J Nucl Med 2000; 41:1357–1362

Hemodynamic abnormality is found in three quarters of patients with carotid artery occlusion (*1*). Severe carotid stenosis decreases regional cerebral blood flow (rCBF). With an inadequate collateral circulation through the circle of Willis, perfusion pressure in the territory of the occluded artery may fall below the lower limit for autoregulation of rCBF. When a maximally dilated arterial bed can no longer maintain rCBF at normal levels, a decline in rCBF starts. In misery perfusion, or an oxygen supply that cannot meet the demand because of decreased rCBF, a compensatory increase in the regional oxygen extraction fraction (rOEF) occurs. If the decrease in rCBF is moderate, the regional cerebral metabolic rate of oxygen ($rCMRO_2$) may be maintained by increased rOEF. Once the reserve of oxygen is exhausted, however, any further transient drop in perfusion pressure decreases $rCMRO_2$ (*2*).

PET with ^{15}O gas is now clinically available to evaluate these pathologic conditions. For chronic occlusive carotid artery disease, revascularization was found to be effective when misery perfusion occurs (*3*). In patients with misery perfusion, improvement of the perfusion pressure by revascularization was found to result in complete cessation of the transient ischemic attack and normalization of the PET finding (*4*). Measurements of $rCMRO_2$ with PET accurately distinguish viable from nonviable cerebral tissue and may be useful in the prospective identification of patients with reversible ischemia (*5*). Hence, PET has proved the most feasible method of evaluating treatment by means of rCBF and oxygen metabolism.

To evaluate other metabolic changes, magnetic resonance spectroscopy (MRS) is also clinically available. MRS has been applied to various pathologic conditions, such as cerebral ischemic injury, brain tumor, and multiple sclerosis (*6–12*). A decline in the *N*-acetyl-aspartate (NAA) concentration indicates a loss of neurons (*7,10,13*). Changes in the levels of choline compounds suggest the destruction of cell membranes (*12*). An increase in the lactate concentration indicates the development of anaerobic glycolysis (*7,10,14,15*). Evaluation of these parameters may provide additional information about biochemical changes in chronic occlusive cerebrovascular diseases. Van der Grond et al. (*16*)

Received Mar. 3, 1999; revision accepted Aug. 4, 1999.

For correspondence or reprints contact: Norihiro Sadato, MD, PhD, Biomedical Imaging Research Center, Fukui Medical University, 23 Shimoaizuki, Matsuoka-cho, Yoshida-gun, Fukui, 910-11 Japan.

examined patients with stenosis of the internal carotid artery before and after endarterectomy with proton MRS. They found that patients without the lactate peak before endarterectomy showed a significant increase in the NAA ratio and recovery to a normal level after endarterectomy. Proton MRS enables a noninvasive chemical analysis in vivo, because the proton is the most sensitive stable nucleus for MRS and almost all metabolites contain protons (*17*). Proton MRS can detect ischemic brain regions by means of changes in metabolites such as lactic acid or NAA, which is believed to be of neuronal origin. However, few MRS studies have examined chronic occlusive cerebrovascular disease.

Carotid occlusive diseases may cause ischemic change in both the gray matter and the white matter as a result of hemodynamic compromise. PET is suitable for evaluation of the oxygen metabolism of the gray matter, whereas MRS can easily be performed on the white matter. The purpose of this study was to validate the applicability of proton MRS for evaluating the carotid occlusive diseases. Metabolic changes in the white matter measured by MRS were compared with the cortical oxygen metabolism and rCBF of the gray matter measured by PET.

MATERIALS AND METHODS

Subjects

Eleven patients with unilateral steno-occlusive carotid artery disease (7 men, 4 women; age range, 54–84 y; mean age, 67.0 y) were included in the study. All patients underwent digital subtraction angiography, MRI, MRS, and PET. To evaluate the ischemic effect on the centrum semiovale and adjacent gray matter, both of which are perfused by the cortical branches of the carotid arteries, we selected the patients with, first, unilateral stenosis or occlusion of the internal carotid artery or unilateral middle cerebral artery stenosis localized in the M1 portion revealed by digital subtraction angiography and, second, no cortical infarction confirmed by MRI. All patients had transient or minor persistent symptoms of ischemic attack in the territory of the middle cerebral artery or internal carotid artery. All patients were examined within 12 wk after the onset of symptoms. Digital subtraction angiography showed that 5 patients had unilateral internal carotid artery occlusion and 4 had internal carotid artery stenosis (>70% reduction). All patients with internal carotid artery occlusion had collateral vessel circulation through the anterior portion of the circle of Willis. Absence of collateral circulation from the vertebrobasilar system through the posterior portion of the circle of Willis was confirmed by digital subtraction angiography. In all patients with internal carotid artery stenosis, the carotid artery distribution of the affected hemisphere was perfused mainly through the stenosed carotid artery. Two other patients showed middle cerebral artery stenosis (>70% reduction) in M1 without any abnormality in the distal portion. The affected region was perfused mainly through the stenosed middle cerebral artery. Absence of cortical infarct was confirmed by absence of anatomic changes indicating cortical infarction by T2-weighted whole-brain MRI and by absence of rCBF defects by PET. Table 1 summarizes the patient data.

Ten age-matched healthy volunteers (3 men, 7 women; age range, 46 to74 y; mean age, 64.3 y), who served as a control group, underwent MRI and MRS. None had ever suffered a cerebral event, and MRI of the brain showed normal findings for all. The ethical committee of Fukui Medical University approved the protocol, and all subjects gave written informed consent for the study. All procedures for both PET and MRS were in accordance with institutional guidelines.

PET Measurement

The PET study was performed using a whole-body PET scanner, Advance (General Electric Medical Systems, Milwaukee, WI). The spatial resolution of the reconstructed clinical PET images is 6 mm full width at half maximum at the center of the field of view, and axial resolution is 4 mm. Before the emission scan, a 10-min transmission scan was obtained using 2 rotating ^{67}Ge–^{68}Ga pin sources for attenuation correction. The tissue activity concentration in the images was cross calibrated against the well counter using a

TABLE 1
Clinical, Radiographic, and PET Data for 11 Patients with Steno-Occlusive Carotid Artery Disease

Patient no.	Age (y)	Sex	Angiography finding	rCBF (mL/100 g/min)		$rCMRO_2$ (mL/100 g/min)		rOEF (mL/100 g/min)		Neurologic signs
				I	C	I	C	I	C	
1	56	M	R ICAS (99)	23.4	27.1	2.52	3.01	0.64	0.55	TIA, multiple
2	60	F	R MCAS (75)	39.7	57.2	2.61	3.71	0.49	0.48	TIA, single
3	65	F	R MCAS (70)	40.1	44.5	3.94	4.13	0.62	0.57	TIA, single
4	68	M	R ICAO	50.6	52.7	3.80	3.90	0.44	0.44	TIA, single
5	66	M	R ICAO	23.5	39.1	1.93	3.07	0.57	0.47	TIA, multiple
6	64	M	R ICAO	33.1	40.6	2.70	3.06	0.50	0.49	Lower limb numbness
7	74	F	L ICAO	42.0	47.1	3.20	3.57	0.49	0.49	TIA, single
8	84	M	L ICAS (99)	47.5	53.6	3.25	3.67	0.52	0.53	TIA, single
9	75	M	R ICAS (90)	29.6	29.3	2.22	2.47	0.50	0.50	Lower limb numbness
10	72	F	R ICAS (90)	47.6	48.4	2.70	2.70	0.43	0.41	TIA, multiple
11	54	M	L ICAO	27.7	35.2	2.45	3.00	0.55	0.53	mild R hemiparesis

I = ipsilateral to affected side; C = contralateral to affected side; ICAS = internal carotid artery stenosis; TIA = transient ischemic attack; MCAS = stenosis of M1 portion of middle cerebral artery; ICAO = internal carotid artery occlusion.

rCBF, $rCMRO_2$, and rOEF are averaged values for 80 regions of interest placed on gray matter in territory of middle cerebral artery and anterior and posterior watersheds. Patient 10 had diabetes mellitus. Values in parentheses are percentage stenosis.

cylindric phantom filled with ^{18}F solution. The head of each subject was immobilized with a head holder and positioned parallel to the canthomeatal line using a light beam. The subjects wore a light, disposable plastic mask and nasal cannula for inhalation of ^{15}O gas produced by a small cyclotron (Oscar 3; Oxford Instruments, Oxon, UK). To calculate rCBF, $rCMRO_2$, and rOEF images, a steady-state inhalation method for ^{15}O-labeled CO, CO_2, and O_2 with intermittent arterial blood sampling was adopted (*18*).

The regions of interest were placed on the gray matter of the affected and unaffected cerebral hemispheres, in the territory of the middle cerebral artery and anterior and posterior watersheds. Eighty circular regions of interest, 6 mm in diameter, were placed on each side. A hemispheric value was calculated as the average of the middle cerebral artery, anterior watershed, and posterior watershed.

MRI and MRS

MRI and proton MRS were performed with a 1.5-T system (Horizon; General Electric Medical Systems). Anatomic MR images were obtained with a T1-weighted sagittal spin-echo sequence (repetition time, 350 ms; echo time, 14 ms) and a T2-weighted transverse fast spin-echo sequence (repetition time, 3500 ms; echo time, 84 ms). The slices were 5 mm thick, and the matrix was 256 × 192.

Proton MRS was performed using the point-resolved spectroscopy pulse sequence (2000/28) with a voxel size of 8 cm^3. All spectra were prescanned with automated software (probe-P; General Electric Medical Systems) that adjusts the radiofrequency, its transit power and water-suppression pulse power, and the magnetic field homogeneity. Volumes of interest were placed in the white matter of the centrum semiovale, for which MR imaging confirmed the absence of infarction. Two volumes of interest were placed in the affected, and 1 in the unaffected, centrum semiovale in the patient group (Fig. 1). For the control group, a volume of interest was placed in the centrum semiovale of 1 side.

The areas of 3 major peaks, including choline (3.2 ppm), the sum of creatine and phosphocreatine (3.0 ppm), and NAA (2.0 ppm), were measured by an automated data analysis package (SA-GE; General Electric Medical Systems) (*19*). No absolute metabolite quantification was attempted, because the peak intensity depends on the acquisition and processing parameters. Instead, all results are given as values relative to the peak of the sum of creatine and phosphocreatine at 3.0 ppm. This peak reflects total creatine concentration, which is constant because of equilibrium between phosphocreatine and free creatine (*20*) and is known to be unchanged during the development of cerebral ischemia and under various pathologic conditions (*8–10,13*).

Data Analyses

An asymmetry index, defined as (ipsilateral − contralateral)/(ipsilateral + contralateral) × 2 × 100%, was used to analyze the relationship between the relative MRS data and the PET value. Statistical significance was assessed with the Mann-Whitney test for comparing the patients' MRS data with that of the healthy volunteers. Linear regression analysis and the Pearson correlation coefficient were used to examine the relationship between the asymmetry index of MRS measurements and that of PET parameters. $P < 0.05$ was considered significant.

RESULTS

Table 1 summarizes the PET measurements. Three patients showed a markedly high cortical rOEF value (>0.56,

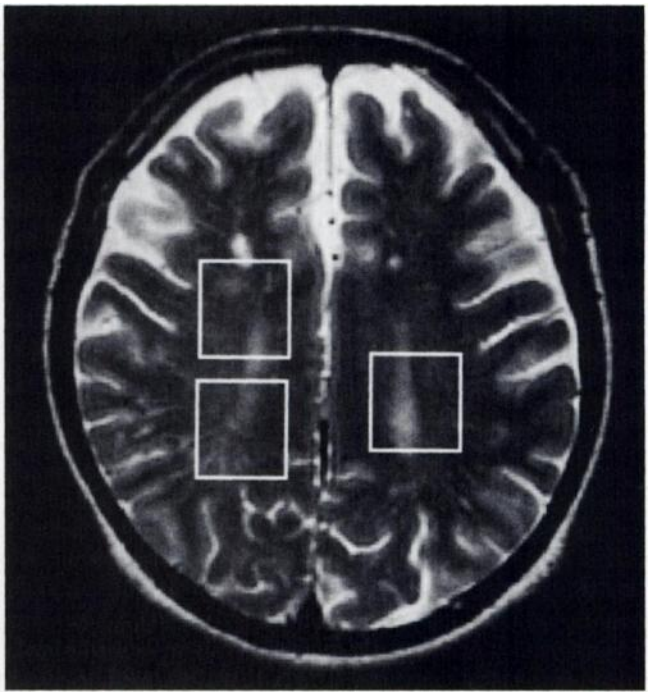

FIGURE 1. Three regions of interest (20 × 20 mm) for proton MRS placed bilaterally in centrum semiovale, 2 on affected side (right) and 1 on unaffected side (left), superimposed on transaxial T2-weighted image of patient 1.

patients 1, 3, and 5). In healthy volunteers, the ratio of NAA to the sum of creatine and phosphocreatine (NAA/Cr) was 1.64 ± 0.13 (mean ± SD) and the ratio of choline to the sum of creatine and phosphocreatine (Cho/Cr) was 0.89 ± 0.07. NAA/Cr and Cho/Cr of the affected hemisphere showed no significant difference. Hence, the values of the 2 volumes of interest were averaged to represent the affected hemisphere. NAA/Cr in the affected hemisphere of patients decreased significantly compared with that of the healthy volunteers ($P < 0.05$), whereas that in the unaffected hemisphere of patients did not. Cho/Cr did not differ significantly between healthy volunteers and patients in either the affected or the unaffected hemisphere. The asymmetry index of NAA/Cr correlated significantly with that of $rCMRO_2$ ($r = 0.77$; $P < 0.01$) and rCBF ($r = 0.73$; $P < 0.05$; Fig. 2; Table 2). No significant correlation was found between the asymmetry index of NAA/Cr and that of rOEF (Table 2). The asymmetry index of Cho/Cr correlated significantly with that of rOEF ($r = 0.65$; $P < 0.05$; Fig. 2) but did not correlate with that of $rCMRO_2$ or rCBF (Table 2). Patients 1 and 5, who experienced multiple transient ischemic attacks, showed the most prominent asymmetry in rOEF and a correlational change in Cho/Cr. Patient 3, who had a single transient ischemic attack, showed a less prominent elevation of rOEF. Patient 5 also showed the most asymmetric decrease in rCBF and $rCMRO_2$ ipsilateral to the affected side. The most prominent asymmetric decrease in Cho/Cr was seen in patient 11, who had mild right hemiparesis (Fig. 2C), causing the correlation coefficient to be less significant (r =

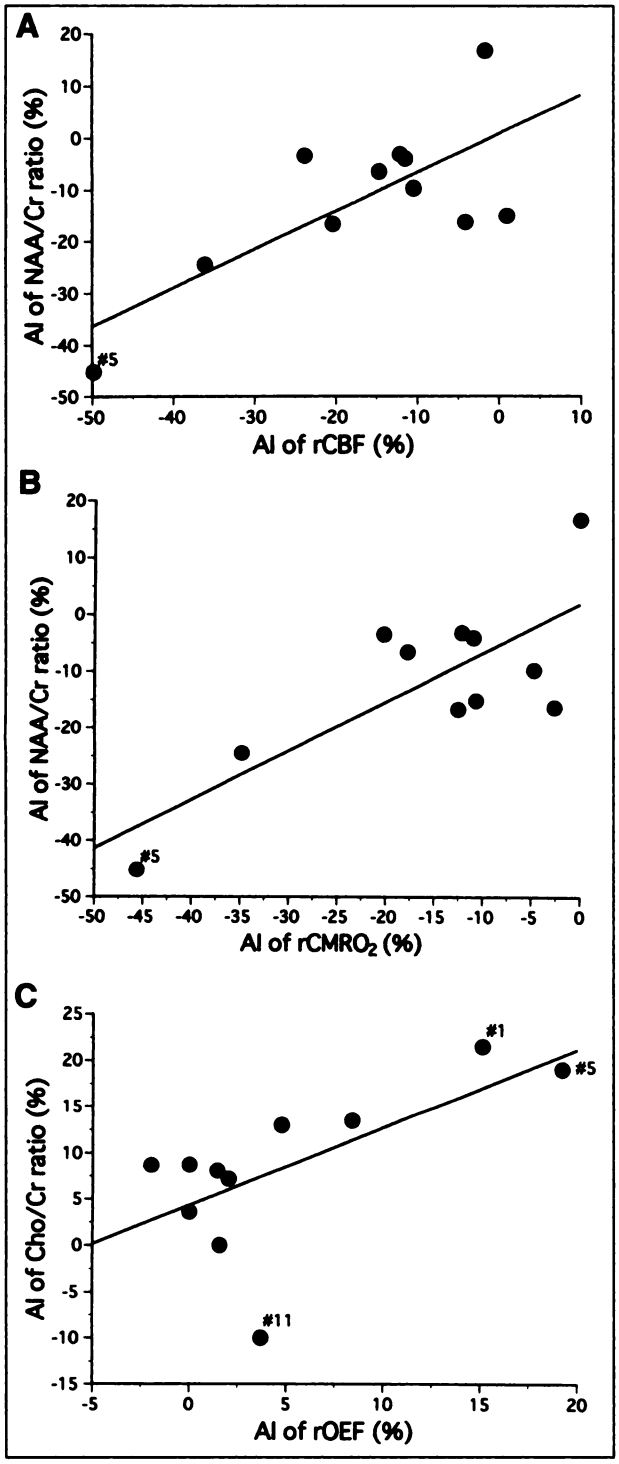

FIGURE 2. Significant positive correlation of asymmetry index of NAA/Cr with that of rCBF ($r = 0.73$; $P < 0.05$) (A) and $rCMRO_2$ ($r = 0.77$; $P < 0.01$) (B). (C) Significant positive correlation of asymmetry index of Cho/Cr with that of rOEF ($r = 0.65$; $P < 0.05$). AI = asymmetry index; #1, #5, and #11 = patients 1, 5, and 11, respectively.

0.65 if patient 11 is included, and $r = 0.84$ if that patient is excluded). Three of 4 patients with a high Cho/Cr on the affected side (>1.03, the mean + 2 SD of the control group) had a markedly increased cortical rOEF value (>0.56) on the same side. In 7 patients with a normal Cho/Cr, the rOEF ranged from 0.44 to 0.55 (mean ± SD = 0.49 ± 0.04) (Fig. 3). In no patient was the peak of lactate, at approximately 1.35 ppm (*20*), distinguishable from other signals in the spectra.

TABLE 2
Correlation Between Percentage Change in Asymmetry Index for MRS and PET

MRS	PET	Correlation coefficient
NAA/Cr	rCBF	0.73*
	$rCMRO_2$	0.77†
	rOEF	0.38
Cho/Cr	rCBF	0.23
	$rCMRO_2$	0.20
	rOEF	0.65*

*$P < 0.05$.
†$P < 0.01$.

DISCUSSION

The centrum semiovale is the deep watershed zone supplied by the distal intraparenchymal penetrating arterioles and is the most distal white matter area perfused by the cortical branches of the carotid arteries. In carotid occlusive diseases, ischemic changes in the deep watershed reflect hemodynamic insufficiency (*21*). The centrum semiovale may be at least as vulnerable as the cortical gray matter to ischemic changes caused by carotid occlusion. Thus, increased rOEF in the gray matter may indicate misery perfusion of both gray and white matter. From a technical point of view, the centrum semiovale is suited for performing accurate spectroscopy of white matter without contamination by gray matter or subcutaneous fat. In PET, the radioactivity in the white matter is sparse because of a lower rCBF in this area, resulting in less accurate parameter estimation, particularly of rOEF, than in gray matter. Hence,

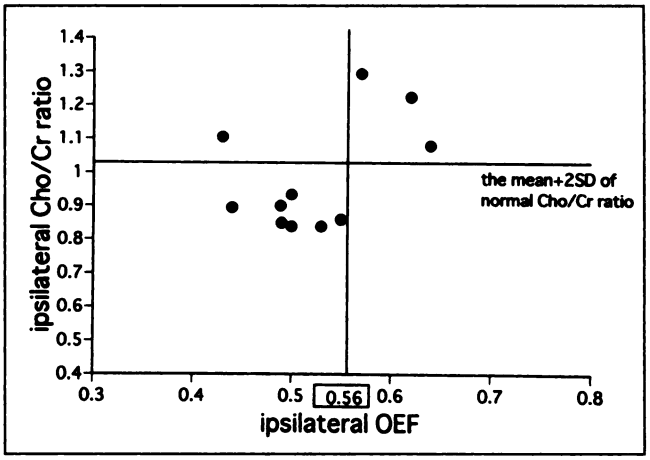

FIGURE 3. Absolute rOEF plotted against Cho/Cr of affected hemisphere. Horizontal line indicates mean + 2 SD of normal Cho/Cr (1.03).

we compared PET measurements of rOEF and $rCMRO_2$ in the gray matter with spectroscopic information obtained from the centrum semiovale.

We used the asymmetry index to determine the relationship between MRS measurements and PET parameters. Powers et al. (*22*) reported that the wide range of normal values for absolute measurements with PET makes detection of abnormalities difficult. The use of hemispheric ratios takes advantage of the basic symmetry of the brain to improve sensitivity for identifying localized disease (*22*). The ratio technique, however, allows only 1 hemisphere to be classified as abnormal and permits no conclusion about the opposite hemisphere. Hemodynamic status in the hemisphere contralateral to a severe carotid stenosis cannot be assumed to be normal, because of the possibility of interhemispheric shunting of blood (*23*), making quantitative measurements important. These 2 methods of analysis therefore complement each other (*22*). On the other hand, rCBF and $rCMRO_2$ in the gray matter decrease with age, whereas rOEF remains fairly stable (*18,24*). Because patient age was not uniform in this study, we applied an asymmetry index to rCBF and $rCMRO_2$, whereas the absolute rOEF was plotted against Cho/Cr.

We have observed that the asymmetry index of NAA/Cr in the centrum semiovale significantly correlated with that of averaged $rCMRO_2$ of gray matter. NAA is an amino acid found almost exclusively in neuronal cells (*6,25*). A consensus is emerging that the level of NAA detected with proton MRS is an index of neuronal viability in brain tissue. NAA is depleted in or absent from infarcted tissue (*7*). $rCMRO_2$, on the other hand, is a good indicator of tissue viability (*26*). Our results indicate that the NAA/Cr of the centrum semiovale may be used as a marker of brain tissue viability. The asymmetry index of NAA/Cr also significantly correlated with that of averaged cortical rCBF. This result may be compatible with the fact that 8 patients showed matched perfusion without an increase in rOEF. In the state of matched perfusion, decreased rCBF correlates with decreased $rCMRO_2$. To confirm whether NAA/Cr reflects $rCMRO_2$, studies that include more patients in the misery perfusion state, in which $rCMRO_2$ is preserved while rCBF decreases, are necessary.

The asymmetry index of Cho/Cr correlated significantly with that of rOEF. Serving as an index of the oxygen carriage reserve, rOEF gives information on the balance between the oxygen supply to the brain and the demand from the brain tissue. Areas with an increased rOEF exhibit poor autoregulation (*27*) or poor CO_2 responsiveness (*28*). At the site of dysautoregulation, rCBF promptly decreases with a reduction in cerebral perfusion pressure. An elevated rOEF implies vulnerability to a reduction in cerebral perfusion pressure and a tendency to develop cerebral infarction because of hemodynamic factors (*29*). Actually, 2 patients with the most prominent asymmetric increase in rOEF in this study experienced multiple transient ischemic attacks. On the other hand, the choline signal in proton MRS in vivo consists predominantly of glycerophosphocholine and phosphocholine (*30*), which are involved in membrane synthesis and degeneration (*31*). Elevation of the choline signal was reported in demyelinating conditions such as multiple sclerosis (*12,32–34*) and adrenoleukodystrophy (*35*). The elevation of choline resonance in these conditions may be caused by the increased visibility of myelin membrane degeneration products, primarily glycerophosphocholine (*35*). An experimental study with primates indicated a transient increase in the choline concentration at the stage of severe vasospasm after subarachnoid hemorrhage, when MRI showed no apparent infarction (*36*). The increase in choline signal intensity preceded the changes in signal intensity shown by T2-weighted MRI in a patient with acute stroke of the middle cerebral artery (*37*). These results indicate that the increase in choline signal intensity is seen in ischemia without apparent morphologic changes on MRI. Free, extracellular choline output from the brain has been shown to increase during focal ischemia (*38–39*). In this study, the increase in Cho/Cr in the centrum semiovale of the affected side may indicate membrane damage caused by chronic ischemia that had not yet developed into apparent morphologic changes. The centrum semiovale may suffer from an ischemic insult at the stage at which the oxygen metabolism of the cerebral cortex is compensated by increased rOEF. This notion is supported by the significant correlation between the Cho/Cr of the centrum semiovale and the cortical rOEF in this study. The correlation in turn indicates that the Cho/Cr of the centrum semiovale may be an indicator of hemispheric rOEF, a good marker for an indication that surgical cerebral revascularization is warranted (*2*).

One patient with a high Cho/Cr and a relatively low rOEF (0.43) by PET had diabetes mellitus (Table 1). Because diabetic patients have an elevated Cho/Cr (*40*), we suppose the high Cho/Cr of this patient was caused by the diabetes mellitus.

No patient showed a lactate peak in this study. The relatively low lactate concentration in normal brain tissue is regarded as an indicator of anaerobic glycolysis (*20*). This finding is consistent with the relatively well maintained $rCMRO_2$ of the patients (Table 1).

CONCLUSION

Metabolic changes revealed in the centrum semiovale by proton MRS can indicate a hemodynamically compromised state and an elevated rOEF in patients with unilateral steno-occlusive carotid artery disease. The anatomic and blood flow changes of ischemia can be evaluated with MRS equipment in clinical settings, adding relevant metabolic information.

ACKNOWLEDGMENT

This study was supported in part by a research grant (JSPS-RFTF97L00203) from the Japan Society for the Promotion of Science.

REFERENCES

1. Powers WJ. Cerebral hemodynamics in ischemic cerebrovascular disease. *Ann Neurol.* 1991;29:231–240.
2. Leblanc R. Physiologic studies of cerebral ischemia. *Clin Neurosurg.* 1991;37:289–311.
3. Muraishi K, Kameyama M, Sato K, et al. Cerebral circulatory and metabolic changes following EC/IC bypass surgery in cerebral occlusive diseases. *Neurol Res.* 1993;15:97–103.
4. Baron JC. Positron tomography in cerebral ischemia: a review. *Neuroradiology.* 1985;27:509–516.
5. Powers WJ, Grubb RL Jr, Darriet D, Raichle ME. Cerebral blood flow and cerebral metabolic rate of oxygen requirements for cerebral function and viability in humans. *J Cereb Blood Flow Metab.* 1985;5:600–608.
6. Birken DL, Oldendorf WH. N-acetyl-L-aspartic acid: a literature review of a compound prominent in ^{1}H-NMR spectroscopic studies of brain. *Neurosci Biobehav Rev.* 1989;13:23–31.
7. Bruhn H, Frahm J, Gyngell ML, Merboldt KD, Hanicke W, Sauter R. Cerebral metabolism in man after acute stroke: new observations using localized proton NMR spectroscopy. *Magn Reson Med.* 1989;9:126–131.
8. Frahm J, Bruhn H, Gyngell ML, Merboldt KD, Hanicke W, Sauter R. Localized proton NMR spectroscopy in different regions of the human brain in vivo: relaxation times and concentrations of cerebral metabolites. *Magn Reson Med.* 1989;11:47–63.
9. Gill SS, Thomas DG, Van Bruggen N, et al. Proton MR spectroscopy of intracranial tumours: in vivo and in vitro studies. *J Comput Assist Tomogr.* 1990;14:497–504.
10. Graham GD, Blamire AM, Howseman AM, et al. Proton magnetic resonance spectroscopy of cerebral lactate and other metabolites in stroke patients. *Stroke.* 1992;23:333–340.
11. Segebarth CM, Baleriaux DF, Luyten PR, den Hollander JA. Detection of metabolic heterogeneity of human intracranial tumors in vivo by ^{1}H NMR spectroscopic imaging. *Magn Reson Med.* 1990;13:62–76.
12. Matthews PM, Francis G, Antel J, Arnold DL. Proton magnetic resonance spectroscopy for metabolic characterization of plaques in multiple sclerosis. *Neurology.* 1991;41:1251–1256.
13. Sappey-Marinier D, Calabrese G, Hetherington HP, et al. Proton magnetic resonance spectroscopy of human brain: applications to normal white matter, chronic infarction, and MRI white matter signal hyperintensities. *Magn Reson Med.* 1992;26:313–327.
14. Houkin K, Kamada K, Kamiyama H, Iwasaki Y, Abe H, Kashiwaba T. Longitudinal changes in proton magnetic resonance spectroscopy in cerebral infarction. *Stroke.* 1993;24:1316–1321.
15. Monsein LH, Mathews VP, Barker PB, et al. Irreversible regional cerebral ischemia: serial MR imaging and proton MR spectroscopy in a nonhuman primate model. *AJNR.* 1993;14:963–970.
16. van der Grond J, Balm R, Klijn CJ, Kappelle LJ, Eikelboom BC, Mali WP. Cerebral metabolism of patients with stenosis of the internal carotid artery before and after endarterectomy. *J Cereb Blood Flow Metab.* 1996;16:320–326.
17. Howe FA, Maxwell RJ, Saunders DE, Brown MM, Griffiths JR. Proton spectroscopy in vivo. *Magn Reson Q.* 1993;9:31–59.
18. Frackowiak RS, Lenzi GL, Jones T, Heather JD. Quantitative measurement of regional cerebral blood flow and oxygen metabolism in man using ^{15}O and positron emission tomography: theory, procedure, and normal values. *J Comput Assist Tomogr.* 1980;4:727–736.
19. Kreis R, Farrow N, Ross BD. Localized ^{1}H NMR spectroscopy in patients with chronic hepatic encephalopathy: analysis of changes in cerebral glutamine, choline and inositols. *NMR Biomed.* 1991;4:109–116.
20. Lewis LD, Ljunggren B, Ratcheson RA, Siesjo BK. Cerebral energy state in insulin-induced hypoglycemia, related to blood glucose and to EEG. *J Neurochem.* 1974;23:673–679.
21. Yamauchi H, Fukuyama H, Yamaguchi S, Miyoshi T, Kimura J, Konishi J. High-intensity area in the deep white matter indicating hemodynamic compromise in internal carotid artery occlusive disorders. *Arch Neurol.* 1991;48:1067–1071.
22. Powers WJ, Press GA, Grubb RL Jr, Gado M, Raichle ME. The effect of hemodynamically significant carotid artery disease on the hemodynamic status of the cerebral circulation. *Ann Intern Med.* 1987;106:27–34.
23. Laurent JP, Lawner PM, O'Connor M. Reversal of intracerebral steal by STA-MCA anastomosis. *J Neurosurg.* 1982;57:629–632.
24. Leenders KL, Perani D, Lammertsma AA, et al. Cerebral blood flow, blood volume and oxygen utilization: normal values and effect of age. *Brain.* 1990;113:27–47.
25. Koller KJ, Zaczek R, Coyle JT. N-acetyl-aspartyl-glutamate: regional levels in rat brain and the effects of brain lesions as determined by a new HPLC method. *J Neurochem.* 1984;43:1136–1142.
26. Powers WJ, Raichle ME. Positron emission tomography and its application to the study of cerebrovascular disease in man. *Stroke.* 1985;16:361–376.
27. Kruse B, Barker PB, van Zijl PC, JH Duyn JH, Moonen CT, Moser HW. Multislice proton magnetic resonance spectroscopic imaging in X-linked adrenoleukodystrophy. *Ann Neurol.* 1994;36:595–608.
28. Kanno I, Uemura K, Higano S, et al. Oxygen extraction fraction at maximally vasodilated tissue in the ischemic brain estimated from the regional CO_2 responsiveness measured by positron emission tomography. *J Cereb Blood Flow Metab.* 1988;8:227–235.
29. Yamauchi H, Fukuyama H, Kimura J, Konishi J, Kameyama M. Hemodynamics in internal carotid artery occlusion examined by positron emission tomography. *Stroke.* 1990;21:1400–1406.
30. Barker PB, Breiter SN, Soher BJ, et al. Quantitative proton spectroscopy of canine brain: in vivo and in vitro correlations. *Magn Reson Med.* 1994;32:157–163.
31. Miller BL. A review of chemical issues in ^{1}H NMR spectroscopy: N-acetyl-L-aspartate, creatine and choline. *NMR Biomed.* 1991;4:47–52.
32. Davie CA, Hawkins CP, Barker GJ, et al. Detection of myelin breakdown products by proton magnetic resonance spectroscopy. *Lancet.* 1993;341:630–631.
33. Posse S, Schuknecht B, Smith ME, van Zijl PC, Herschkowitz N, Moonen CT. Short echo time proton MR spectroscopic imaging. *J Comput Assist Tomogr.* 1993;17:1–14.
34. Miller DH, Austin SJ, Connelly A, Youl BD, Gadian DG, McDonald WI. Proton magnetic resonance spectroscopy of an acute and chronic lesion in multiple sclerosis. *Lancet.* 1991;337:58–59.
35. Oppenheimer SM, Bryan RN, Conturo TE, Soher BJ, Preziosi TJ, Barker PB. Proton magnetic resonance spectroscopy and gadolinium-DTPA perfusion imaging of asymptomatic MRI white matter lesions. *Magn Reson Med.* 1995;33:61–68.
36. Handa Y, Kaneko M, Matuda T, Kobayashi H, Kubota T. In vivo proton magnetic resonance spectroscopy for metabolic changes in brain during chronic cerebral vasospasm in primates. *Neurosurgery.* 1997;40:773–780
37. Barker PB, Gillard JH, van Zijl PC, et al. Acute stroke: evaluation with serial proton MR spectroscopic imaging. *Radiology.* 1994;192:723–732.
38. Jope RS, Jenden DJ. Choline and phospholipid metabolism and the synthesis of acetylcholine in rat brain. *J Neurosci Res.* 1979;4:69–82.
39. Scremin OU, Jenden DJ. Focal ischemia enhances choline output and decreases acetylcholine output from rat cerebral cortex. *Stroke.* 1989;20:92–95.
40. Kreis R, Ross BD. Cerebral metabolic disturbances in patients with subacute and chronic diabetes mellitus: detection with proton MR spectroscopy. *Radiology.* 1992;184:123–130.